**[Supplement]**
**Artificial intelligence-Enhanced Quantitative Ultrasound for Breast Cancer: Pilot Study on Quantitative Parameters and Biopsy Outcomes.**

**Supplementary Table 1. Training objective.**

| **Algorithm 1** Optimization |
| --- |
| **Input:** $(RF, cond, I_{cond})\sim \mathcal{D}ataset$ |
| **Initialize**: neural network $parameter$: $\theta$ |
| 1: **For** it **in** iterations **do** |
| 2: Split $Dataset_{train}$ $and$ $Dataset_{test} \leftarrow Dataset$ |
| 3: **Composed train batch:** L$(RF_{tr}, cond_{tr}, I_{cond_{Tr}})\sim Dataset_{train}$ |
| 4: **Calculate loss:** Meta DSA loss $L_{QI}$ $(RF_{tr}, cond_{tr}, I_{cond_{Tr}})$ |
| 5: **Model Optimization** $\theta = \theta - \lambda \frac{\partial\left(L_{QI}\,(RF_{tr}, cond_{tr}, I_{cond_{Tr}})\right)}{\partial\theta}$ |
| 6: **end for** |

The optimization procedure of the proposed quantitative imaging neural network is introduced in Algorithm 1 (Supplementary Table1).
The 16.5k datasets are spitted into the train (n=15.5k) and test (n=1.0k) datasets. Each data is composed of a radio-frequency signal, condition variable ($cond$), and ground truth quantitative image ($I_{cond}$). A batch of size 8 is configured for the training of the neural network. The learning objective of the system is described as follows:

$$\theta^* = arg\min_{\theta}\ \mathrm{E}_{\mathcal{D}ataset}[\|I_{cond} - \theta(RF, cond)\|^2] + L_R + L_2, \quad (1)$$

$$where, \qquad L_R = \sum_R [\|y_R - \theta_R(RF, cond)\|^2]$$

$$and\ , \qquad L_2 = \sum_i w_i^2$$

The neural network tries to minimize the squared difference between the neural network output $\theta(RF, cond)$ and corresponding ground truth $I_{cond}$. $L_R$ is employed to parameterize each resolution subnetwork. The $L_2$ regularized the weight $w_i$ of convolutional layers, and prevents the neural network from over-fitting.

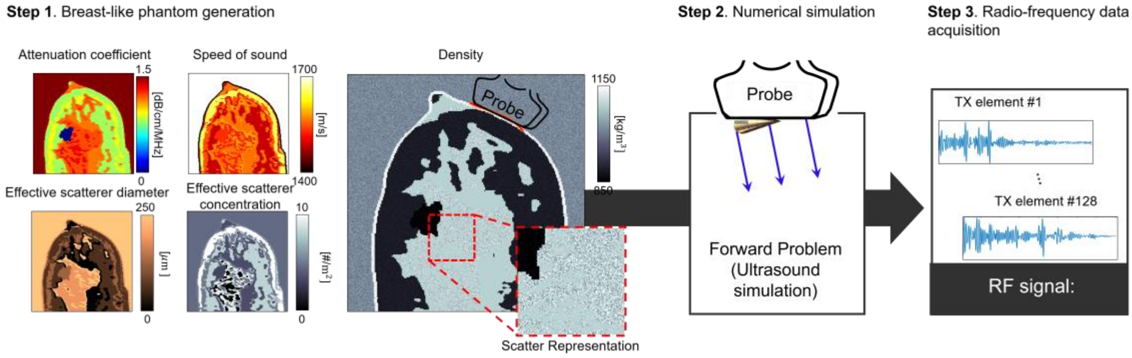


**Supplementary Figure 1. Illustration of the numerical ultrasonic simulation**

Breast-tissue mimicking acoustic phantoms are modeled to simulate ultrasonic wave propagation. The anatomy of the phantom is generated using a number of MRI-driven realistic breast tissue segments (UWCEM breast phantom repository [8]). The shape of the breast tumor is modeled using breast b-mode images of 600 female subjects with malignant (N=210) and benign (N=445) lesions [9]. The wave propagation property is set to cover generality soft tissue biomechanical characteristics. The probe is placed along the skin layer and the region of interest of size 50×50mm is configured correspondingly. The ultrasound simulation is implemented using the k-wave simulation toolbox in MATLAB and imitates ultrasound measurement of 128 elements, 5MHz linear probe. Through the simulation, a radio-frequency signal of each 128 probe elements is obtained, and configure the dataset for the training of the neural network.

**Supplementary Figure 2. Bio-mechanical properties considered in the proposed quantitative imaging system.**

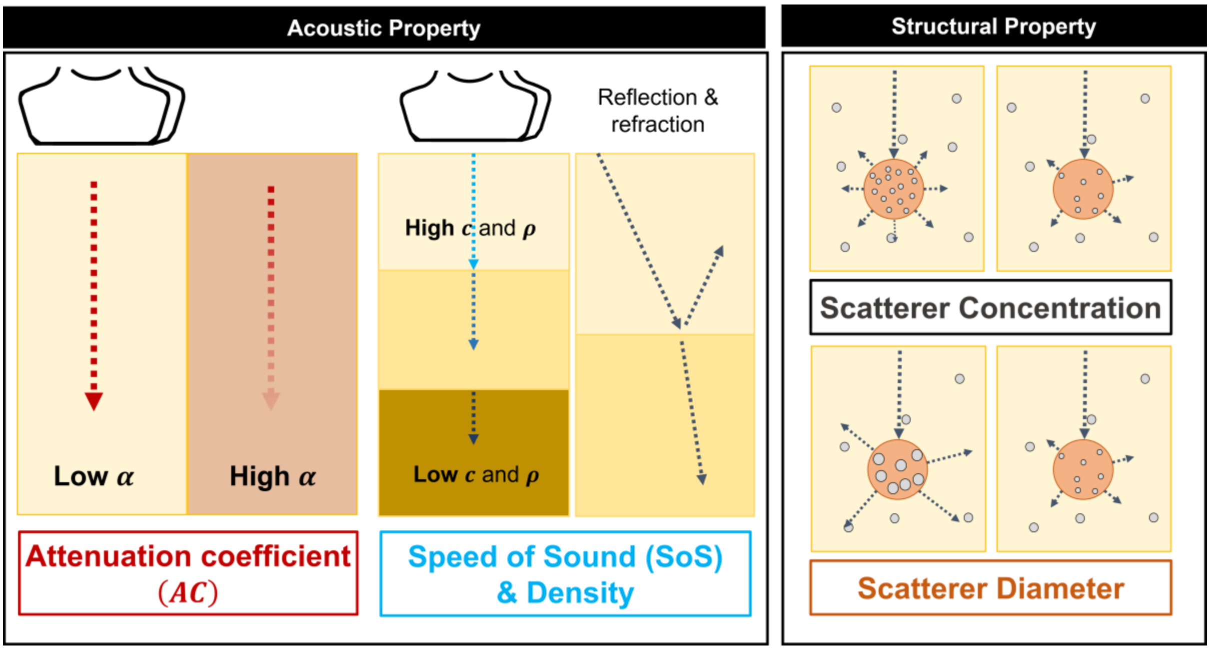


**Supplementary Figure 1. Bio-mechanical properties considered in the proposed quantitative imaging system.**

Tissue biomechanical characteristics affecting ultrasound wave propagation are divided into two categories, which are acoustic and structural properties. Tissue attenuation coefficient, speed of sound, and density are considered acoustic properties that determine how the tissue interact with ultrasound wave. The attenuation coefficient is the degree of which ultrasound waves are attenuated in tissue. Hence, the tissue attenuation coefficient is related to the amplitude of the radio-frequency signal. The speed of sound in fluences the propagation speed of ultrasound wave. The tissue speed of sound determines the arrival time of the pulse-echo signal and is reflected in the phase of the received ultrasound signal. The tissue density formulates acoustic impedance in conjunction with sound speed. The acoustic properties regulate the reflection and refraction of an ultrasound pulse in heterogeneous tissue. The scattering of ultrasonic waves occurs due to the heterogeneity of speed of sound and density in tissue, and the size and concentration of the scattering body that determines the scattering of ultrasonic waves are considered as structural properties. The geometry of micro-tissue components governs the ultrasound scattering effect, and such tissue structural properties are recognized by analyzing envelop statistics of the received ultrasound signal. The proposed quantitative imaging system is configured to reconstruct the tissue attenuation coefficient, speed of sound, and scattering feature of the tissue, by analyzing amplitude, phase, and envelop statistics of the radio-frequency signal, respectively.

**Implementation details**

The proposed quantitative imaging system is accelerated with Geforce RTX 3090 Ti (Nvidia, US) graphics processing unit. The neural network was optimized with the stochastic gradient descent method using Adam [8] with a learning rate $1^{e-4}$ ( $\beta_1$= 0.9, $\beta_2$ = 0.999). The neural network is trained up to 120 epochs, which is determined based on the convergence of validati on dataset assessed mean normalized absolute error (MNAE), peak signal-to-noise ratio (PSNR ), and structural similarity index (SSIM) metrics. Dropout [9] with a retention probability of 0.5 is implemented for the generalization of the neural network

**References**


[1] M. J. Burfeindt, T. J. Colgan, R. O. Mays, J. D. Shea, N. Behdad, B. D. Van Veen, and S. C. Hagness, "MRI-derived 3D-printed breast phantom for microwave breast imaging validation," IEEE Antennas and Wireless Propagation Letters, vol. 11, pp. 1610-1613, 2012.

[2] Al-Dhabyani W, Gomaa M, Khaled H, Fahmy A. Dataset of breast ultrasound images. Data in Brief. 2020 Feb;28:104863. DOI: 10.1016/j.dib.2019.104863.

[3] DUMOULIN, Vincent; SHLENS, Jonathon; KUDLUR, Manjunath. A learned representation for artistic style. arXiv preprint arXiv:1610.

[4] Wang, J., Sun, K., Cheng, T., Jiang, B., Deng, C., Zhao, Y., ... & Xiao, B. (2020). Deep high-resolution representation learning for visual recognition. IEEE transactions on pattern analysis and machine intelligence, 43(10), 3349-3364.

[5] He, Kaiming, et al. "Deep residual learning for image recognition." Proceedings of the IEEE conference on computer vision and pattern recognition. 2016.

[6] Li C, Duric N, Littrup P, Huang L. In vivo breast sound-speed imaging with ultrasound tomography. Ultrasound Med Biol. 2009 Oct;35(10):1615-28. doi: 10.1016/j.ultrasmedbio.2009.05.011. Epub 2009 Aug 3. PMID: 19647920; PMCID: PMC3915527.

[7] Ruby L, Sanabria SJ, Martini K, Dedes KJ, Vorburger D, Oezkan E, Frauenfelder T, Goksel O, Rominger MB. Breast Cancer Assessment With Pulse-Echo Speed of Sound Ultrasound From Intrinsic Tissue Reflections: Pro of-of-Concept. Invest Radiol. 2019 Jul;54(7):419-427. doi: 10.1097/RLI.0000000000000553. PMID: 30913054.

[8] KINGMA, Diederik P.; BA, Jimmy. Adam: A method for stochastic optimization. arXiv preprint arXiv:1412.6980, 2014.

[9] Srivastava, N., Hinton, G., Krizhevsky, A., Sutskever, I., & Salakhutdinov, R. (2014). Dropout: a simple way to prevent neural networks from overfitting. The journal of machine learning research, 15(1), 1929-1958.